Protein Kinase D1 Is Essential for Contraction-induced Glucose Uptake but Is Not Involved in Fatty Acid Uptake into Cardiomyocytes

THE JOURNAL OF BIOLOGICAL CHEMISTRY VOL. 287, NO. 8, pp. 5871–5881, February 17, 2012

Protein Kinase D1 Is Essential for Contraction-induced Glucose Uptake but Is Not Involved in Fatty Acid Uptake into Cardiomyocytes*[S]

Received for publication, July 12, 2011, and in revised form, December 8, 2011 Published, JBC Papers in Press, December 9, 2011, DOI 10.1074/jbc.M111.281881

Ellen Dirkx[‡], Robert W. Schwenk[‡], Will A. Coumans[‡], Nicole Hoebers[‡], Yeliz Angin[‡], Benoit Viollet[§], Arend Bonen[¶], Guillaume J. J. M. van Eys[‡], Jan F. C. Glatz[‡], and Joost J. F. P. Luiken[‡1]

From the [‡]Department of Molecular Genetics and Cardiovascular Research Institute Maastricht, Maastricht University, Maastricht 6200 MD, The Netherlands, the [§]Institut Cochin INSERM U1016, CNRS UMR 8104, Université Paris Descartes, Sorbonne Paris Cité, 75014 Paris, France, and the [¶]Department of Human Health and Nutritional Sciences, College of Biological Sciences, University of Guelph, Guelph, Ontario N1G 2W1, Canada

Background: Contraction of cardiomyocytes up-regulates glucose and fatty acid uptake by GLUT4 and CD36 translocation to the sarcolemma.
Results: Silencing of protein kinase D1 abolishes contraction-induced GLUT4 but not CD36 translocation.
Conclusion: Protein kinase D1 signaling mediates cardiac glucose but not fatty acid uptake.
Significance: Selective stimulation of glucose uptake is beneficial for diabetic hearts characterized by elevated fatty acid uptake.

Increased contraction enhances substrate uptake into cardiomyocytes via translocation of the glucose transporter GLUT4 and the long chain fatty acid (LCFA) transporter CD36 from intracellular stores to the sarcolemma. Additionally, contraction activates the signaling enzymes AMP-activated protein kinase (AMPK) and protein kinase D1 (PKD1). Although AMPK has been implicated in contraction-induced GLUT4 and CD36 translocation in cardiomyocytes, the precise role of PKD1 in these processes is not known. To study this, we triggered contractions in cardiomyocytes by electric field stimulation (EFS). First, the role of PKD1 in GLUT4 and CD36 translocation was defined. In PKD1 siRNA-treated cardiomyocytes as well as cardiomyocytes from PKD1 knock-out mice, EFS-induced translocation of GLUT4, but not CD36, was abolished. In AMPK siRNA-treated cardiomyocytes and cardiomyocytes from AMPKα2 knock-out mice, both GLUT4 and CD36 translocation were abrogated. Hence, unlike AMPK, PKD1 is selectively involved in glucose uptake. Second, we analyzed upstream factors in PKD1 activation. Cardiomyocyte contractions enhanced reactive oxygen species (ROS) production. Using ROS scavengers, we found that PKD1 signaling and glucose uptake are more sensitive to changes in intracellular ROS than AMPK signaling or LCFA uptake. Furthermore, silencing of death-activated protein kinase (DAPK) abrogated EFS-induced GLUT4 but not CD36 translocation. Finally, possible links between PKD1 and AMPK signaling were investigated. PKD1 silencing did not affect AMPK activation. Reciprocally, AMPK silencing did not alter PKD1 activation. In conclusion, we present a novel contraction-induced ROS-DAPK-PKD1 pathway in cardiomyocytes. This pathway is activated separately from AMPK and mediates GLUT4 translocation/glucose uptake, but not CD36 translocation/LCFA uptake.

Cardiac substrate utilization is predominantly regulated by GLUT4 and CD36, the main cardiac transporters for glucose and long chain fatty acids (LCFA),[2] respectively (1). In addition to being present at the sarcolemma, GLUT4 and CD36 are also stored in endosomal compartments, from where these transporters can be translocated to the sarcolemma. GLUT4 translocation is known to be a vesicle-mediated process depending on, a.o., coat, and SNARE proteins. Recently, both groups of proteins have also been found to mediate CD36 translocation (2). Alterations in contraction are an important denominator of cardiac substrate utilization. Increased contraction enhances the demands for glucose and LCFA, and accordingly, GLUT4 and CD36 have been found to translocate to the sarcolemma under this condition (1, 3).

The signaling pathways involved in contraction-induced GLUT4 and CD36 translocation in the heart have been incompletely charted. Contraction signaling is under control of the cardiac energy status, and particularly sensitive to increases in intracellular levels of AMP (4). AMP binds to the regulatory γ-subunit of the heterotrimeric enzyme AMP-activated protein kinase (AMPK). This binding allosterically further stimulates activity of AMPK phosphorylated at Thr^{172} within the catalytic α-subunit by the upstream kinase LKB1, and simultaneously inhibits Thr^{172} dephosphorylation (4). Both LKB1 and AMPK have been shown to be necessary for GLUT4 and CD36 translocation in cardiomyocytes (5, 6). However, it is not known whether there are also kinases that are differentially involved in contraction-induced GLUT4 and CD36 translocation in the heart.

Another contraction-activated kinase in the heart is protein kinase D1 (PKD1). Contraction stimulation has recently been

* This work was supported by the Transnational University Limburg and European Community Integrated Project LSHM-CT-2004-005272 (Exgenesis).
[S] This article contains supplemental Figs. S1–S3.
[1] To whom correspondence should be addressed: P.O. Box 616, 6200 MD Maastricht, the Netherlands. Tel.: 31-433881998; Fax: 31-433884574; E-mail: j.luiken@maastrichtuniversity.nl.

[2] The abbreviations used are: LCFA, long chain fatty acid; PKD1, protein kinase D1; AMPK, AMP-activated protein kinase; EFS, electric field stimulation; ROS, reactive oxygen species; DAPK, death-activated protein kinase; MPG, *N*-(2-mercaptopropionyl)glycine; nc, noncoding; ara-A, 9-β-D-arabinofuranoside; AICAR, 5-aminoimidazole-4-carboxamide-1-β-D-ribofuranoside.

found to autophosphorylate PKD1 at Ser^{916}, resulting in increased phosphorylation of established PKD target proteins (7). PKD1 is the founding member of the PKD family, a novel family of protein kinase C-related Ser/Thr kinases. PKD1 is associated with a number of cellular processes. For instance, PKD1 is involved in translocation of secretory proteins from the Golgi to the plasma membrane in secretory cells (8). Additionally, PKD1 links increased production of reactive oxygen species (ROS) to inflammatory responses through activation of nuclear factor κB (9). Previously, we discovered that PKD1 is linked to contraction-induced glucose uptake (7). However, the pharmacological agents used to inhibit PKD additionally inhibited PKC members and a variety of other kinases (7). Hence, the role of PKD1 in contraction-induced GLUT4 translocation awaits more definite proof. Furthermore, the role of PKD1 in contraction-induced CD36 translocation is unknown.

In this study, we examined the role of PKD1 in glucose and LCFA uptake in contracting cardiomyocytes and compared the effects of PKD1 with those of AMPK in inducing GLUT4 and CD36 translocation. Furthermore, we mapped the signaling events upstream of PKD1, focusing on ROS as candidate second messenger. Finally, we investigated whether or not PKD1 signaling converges with AMPK signaling in regulation of contraction-induced substrate uptake in the heart. For manipulation of PKD1 and AMPK expression, we used the cardiac cell line HL1, in which we knocked down PKD1 and AMPK via siRNA technology. We also used cardiomyocytes from cardiospecific PKD1 and AMPKα2 knock-out mice. For inhibition and activation of ROS signaling, we treated primary rat cardiomyocytes with *N*-(2-mercaptopropionyl)glycine (MPG) and H_2O_2, respectively. We conclude that upon contraction-induced ROS production, PKD1 becomes activated and induces GLUT4, but not CD36 translocation, separately from AMPK.

EXPERIMENTAL PROCEDURES

Animals—Male Lewis rats (200–250 g) were obtained from Charles River. Mice with a conditioned PKD1-null allele were generously provided by Prof. E. N. Olson (Dallas, TX) and cross-bred with transgenic mice with a Cre-recombinase gene under a αMHC promoter (Fielitz PNAS 2008). Knock-out mice in which the AMPKα2 catalytic subunit gene was inactivated were derived from one of our laboratories (10). All of the animals were maintained at the Experimental Animal Facility of Maastricht University. The investigation conforms to the Guide for Care and Use of Laboratory Animals published by the United States National Institutes of Health (Publication No. 85-23, revised 1996).

Materials—Lipofectamine 2000, MPG, and 5-(and −6)-carboxy-2′,7′-dichlorodihydrofluorescein diacetate were purchased from Invitrogen. Liberase blendzyme 1, complete protease inhibitor, and PhosSTOP phosphatase inhibitor were obtained from Roche Applied Science. Igepal CA-630 was from Sigma. siRNAs against PKD1 (GGAGGGUGAUCUCAUUGAAtt), AMPKα2 catalytic subunit (GCACGGUCAAGUUUUGAUUtt), and DAPK1 (GCAAGAAACAUUAGCGAAUtt), were obtained from Ambion Applied Biosystems (Austin, TX). The plasmid coding for GLUT4myc was kindly provided by Dr. J. Eckel (German Diabetes Center, Düsseldorf, Germany). GFP eukaryotic expression vector pEGFP-N1 was from Clontech. Antibodies directed against phospho-PKD/PKC-μ (Ser^{916}), phospho-AMPK (Thr^{172}), GAPDH, caveolin 3, and the Myc epitope were obtained from Cell Signaling (Beverly, MA), and the antibody directed against DAP kinase-1 was purchased from Sigma-Aldrich. The antibody directed against GLUT4 was obtained from Santa Cruz Biotechnology (Santa Cruz, CA), and the antibody against mouse CD36 was from Chemicon (Billerica, MA). Protein G-Sepharose beads were from GE Healthcare.

Experimental Procedures on HL-1 Atrial Cardiomyocytes—HL-1 cells were kindly provided by Dr. Claycomb (Louisiana State University, New Orleans, LA) and cultured as previously described (2). HL1 cells were transfected with noncoding (nc)-, PKD1-, AMPK-, or DAPK1-siRNA and cotransfected with pCMV-GLUT4myc (in case of sarcolemmal GLUT4 detection). Transfection of siRNA was done by mixing 200 pmol of siRNA with 8 μl of Lipofectamine 2000/well (6-well plate) in antibiotic- and norepinephrine-free culture medium. After 6 h, the medium was changed to regular culture medium. After 48 h, the medium was changed to FCS- and norepinephrine-free medium overnight. Subsequently, the cells were subjected to electric field stimulation (EFS) for inducing controlled cellular contractions (in case of substrate uptake studies and transporter translocation assays) or subjected to oligomycin treatment (in case of verification of loss of signaling caused by silencing of each of the three kinases). In case of EFS, the C-Pace stimulator from IonOptix (Milton, MA) was used at a setting of 40 V, 5-ms pulse duration, and 2 Hz for 30 min. In case of oligomycin, the cells were incubated for 30 min at 1 μM. Immediately thereafter, the following parameters were measured: expression and phosphorylation of PKD1 and AMPK (6, 7); sarcolemmal contents of CD36 and GLUT4myc; uptake of glucose and LCFA; and microscopical detection of GLUT4 translocation. For detection of total and phosphorylated PKD1 and AMPK, the cells were lysed in Laemmli sample buffer and then subjected to immunoblotting (see below).

In case of sarcolemmal CD36 detection, the cells were incubated with an anti-CD36 antibody (1:2,000 in blocking buffer) for 30 min at room temperature and subsequently washed three times with blocking buffer. Next, the cells were incubated with a HRP-linked secondary antibody (1:4,000 in blocking buffer) for 30 min at room temperature. After extensive washing with blocking buffer and then with PBS, an *ortho*-phenylenediamine-H_2O_2 solution was added as a substrate for the bound HRP. The reaction was carried out at room temperature and stopped after 30 min by the addition of 1 M H_2SO_4. Color development, representative of the amount of CD36 present at the plasma membrane, was quantified by measurement of the absorbance at 490 nm. The background signal of the control (incubation without primary antibody) was subtracted from the raw data. In case of sarcolemmal GLUT4myc detection, HL1 cells were cotransfected with a plasmid coding for GLUT4myc (11) simultaneously with the transfection with the selected siRNAs. The staining of plasmalemmal GLUT4myc is done with a primary antibody against Myc and an appropriate HRP-linked secondary antibody. Furthermore, the GLUT4myc surface staining is homologous to the method of CD36 cell surface staining.

For measurement of substrate uptake, palmitate (coupled to BSA in a palmitate:BSA ratio of 1:3) and deoxy-D-glucose were added to final concentrations of 20 and 4 μM, respectively, with tracer amounts of [^{14}C]palmitate and 2-deoxy-D-[^{3}H]glucose. After 10 min, uptake was terminated, and unbound substrate was removed by washing the cells with ice-cold depletion medium containing 0.2 mM phloretin. After transfer of the glass slides into new culture dishes, the cells were lysed by the addition of 1 M NaOH. Subsequently, incorporated glucose and palmitate were measured by scintillation counting of ^{14}C and ^{3}H.

To microscopically track GLUT4 translocation, murine GLUT4 cDNA was ligated into pEGFP-N1. The resulting plasmid was transfected into HL1 cells using Lipofectamine 2000. Transfected cells were observed and photographed by a Leica TCS SPE confocal scanning microscope.

Isolation and Treatment of Adult Rat and Mouse Cardiomyocytes—Cardiomyocytes were isolated from male Lewis rats (200–250 g) (12) or from male and female WT or transgenic C57BL/6 mice (6) using a Langendorff perfusion system and a Krebs Henseleit bicarbonate medium equilibrated with a 95% O_2, 5% CO_2 gas phase at 37 °C. Cardiomyocytes were incubated at 37 °C with continuous shaking. Rat cardiomyocytes were subjected to EFS at 40 V, 5-ms pulse duration, 4 Hz for 6 min. Mouse cardiomyocytes underwent EFS at 40 V, 10 ms, 2 Hz for 4 min. Furthermore, rat or mouse cardiomyocytes were incubated for 15 min at 37 °C with 5 or 1 μM oligomycin, respectively. For EFS, a IonOptix stimulator was used. In case of addition of pharmacological inhibitors, compounds were added 30 min prior to stimulation. Immediately after stimulation, a mixture of [^{3}H]deoxyglucose and [^{14}C]palmitate was added, and uptake of these substrates was determined during 5 min as pellettable radioactivity in a similar manner as described for HL1 cells, with the difference that the cells were washed by low speed centrifugation followed by lysis directly in scintillation fluid.

Immunoprecipitation—Cardiomyocytes were pelleted and incubated for 1 h in ice-cold lysis buffer (50 mM Tris-HCl, pH 7.4, 150 mM NaCl, 1% Igepal CA-630, 0.5% sodium deoxycholate, 0.1% SDS, complete protease inhibitor, and PhosSTOP phosphatase inhibitor). Cell lysates were pelleted, and the supernatant fractions were incubated with antibody (5 μg) overnight at 4 °C. 50 μl of protein G-Sepharose beads was added, and incubations were continued for 1 h at 4 °C. The beads were collected by pulse centrifugation and washed. The final pellet was resuspended in 30 μl of Laemmli sample buffer and heated to 95 °C for 5 min. The beads were pelleted by centrifugation, and the supernatant was used for Western blot analysis.

Immunoblotting—Proteins were separated by SDS-PAGE on 4–12% Bis-Tris Criterion XT precast gels (Bio-Rad) and transferred to nitrocellulose membranes. The membranes were probed with the relevant primary antibodies according to the manufacturer's instructions. The protein bands were visualized using enhanced chemiluminescence, and immunoblot intensities were quantitatively analyzed using Bio-Rad Quantity One software (7).

Flow Cytometry Analysis—Cardiomyocytes were incubated for 30 min with 10 μM 5-(and 6)-carboxy-2′,7′-dichlorodihydrofluorescein diacetate. Afterward, the cardiomyocytes were washed with PBS, and fluorescence was analyzed by flow cytometry.

Statistics—All of the data are presented as the means ± S.E. Statistical analysis was performed by using Student's *t* test or analysis of variance (including Newman-Keuls multiple comparison test) and statistical analysis software Prism 4 (GraphPad Software, Inc.). A p value of <0.05 was considered statistically significant.

RESULTS

Involvement of PKD1 and AMPK in Contraction-induced Glucose and LCFA Uptake—HL1 cardiomyocytes were chosen as model to study the influence of PKD1 and AMPK on cardiac substrate uptake. This cell line is capable of contracting in an electric field (2). Additionally, we verified in HL1 cells that GLUT4 translocation is entirely responsible for stimulus-induced glucose uptake and CD36 translocation for stimulus-induced LCFA uptake (2). Furthermore, HL1 cells can be readily manipulated with siRNA technology for protein silencing (2).

Treatment of HL1 cells with siRNA against PKD1 or AMPK resulted in a 40–50% specific loss of protein expression of each of these kinases (Fig. 1*A*). Oligomycin, an inhibitor of mitochondrial F_1F_0-ATPase, has been previously shown to stimulate AMPK and PKD activation in a similar manner as does contraction (3, 7) and was used in these experiments as stimulus to verify whether the down-regulation of synthesis of both kinases would also reduce their activation. Silencing of PKD1 resulted in a complete loss of oligomycin-induced PKD1-Ser^{916} phosphorylation, and silencing of AMPK led to a complete loss of oligomycin-induced AMPK-Thr^{172} phosphorylation. (Fig. 1*A*). Furthermore, PKD1 silencing did not affect AMPK activation, and conversely, AMPK silencing did not influence PKD1 activation, indicating that these kinases operate in separate pathways (Fig. 1*A*).

The role of PKD1 in contraction-induced GLUT4 and CD36 translocation was assessed by fluorometric assessment of the cell surface presence of GLUT4myc and CD36 We observed that oligomycin treatment and EFS enhanced the sarcolemmal abundance of both transporters (Fig. 1*B*). PKD1 silencing abrogated the increase in cell surface content of GLUT4, but not of CD36 (Fig. 1*B*). In line with these findings, PKD1 silencing abrogated oligomycin-induced glucose uptake, but not LCFA uptake, into HL1 cells (Fig. 1*B*). The involvement of PKD1 in contraction-induced GLUT4 translocation was visualized using a GLUT4-GFP hybrid protein. GLUT4-GFP was shown to be translocated to the sarcolemma upon EFS, and this was abolished by PKD1 silencing (Fig. 1*C*).

Contrary to PKD1, AMPK knockdown in HL1 cells inhibited EFS-induced translocation of both GLUT4 and CD36 (Fig. 1*D*). AMPK silencing also caused a modest increase in basal CD36 presence at the sarcolemma.

Given that the knockdowns of both PKD1 and AMPK were partial (~50%), it is of note that the inhibitory effects of these knockdowns on oligomycin/contraction-induced GLUT4 or

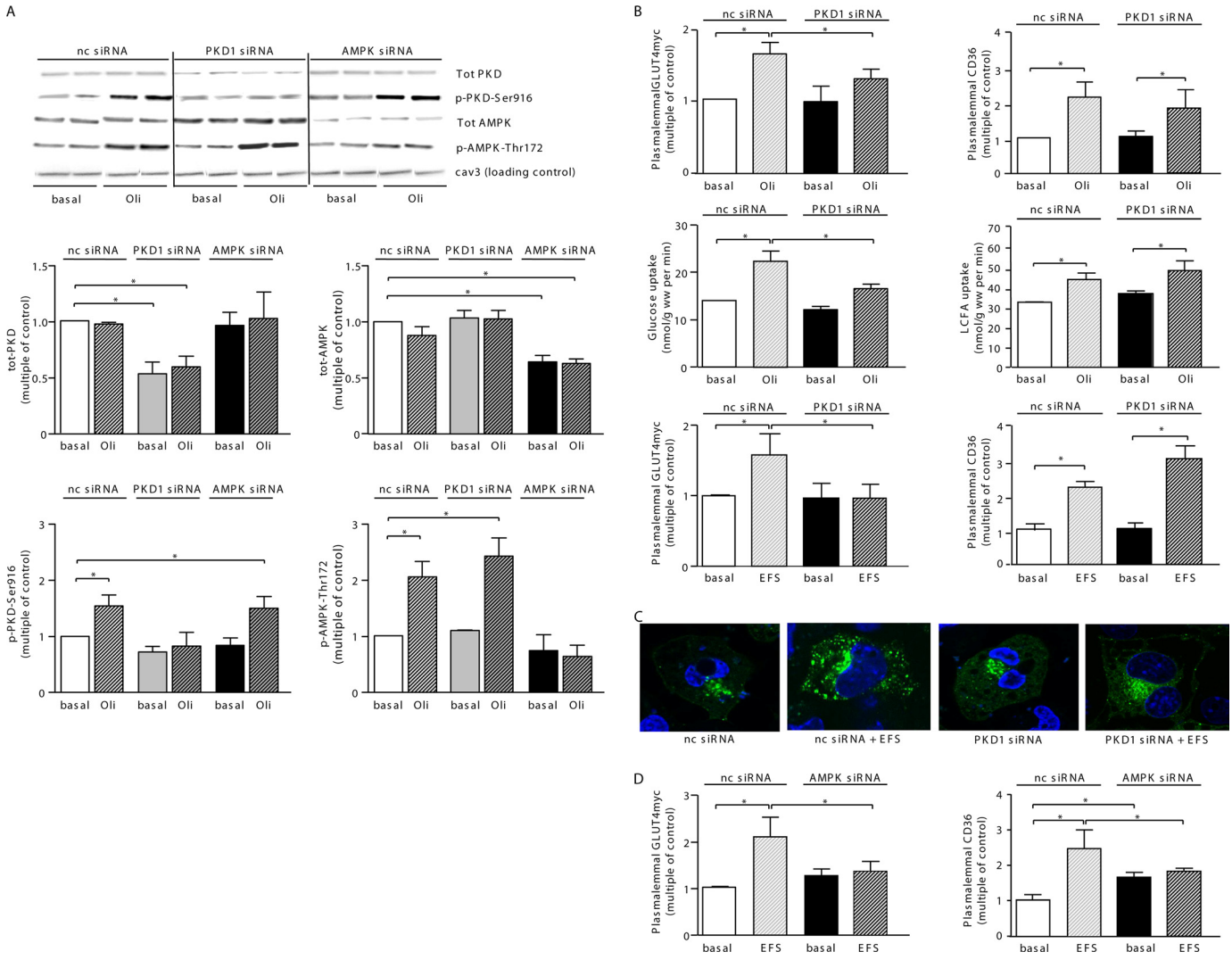

FIGURE 1. **PKD1 silencing in HL1 cardiomyocytes abolishes contraction-induced GLUT4 translocation and glucose uptake but not AMPK activation or CD36 translocation and LCFA uptake.** HL1 cardiomyocytes were transfected with noncoding (nc)-, PKD1-, or AMPK-siRNA (and cotransfected with pCMV-GLUT4myc in case of sarcolemmal GLUT4 detection). After 48 h, the cells were treated with oligomycin (*Oli*; 1 μM, 30 min) or subjected to EFS for 30 min and subsequently used for analysis of PKD1 and AMPK signaling, GLUT4 and CD36 translocation, glucose, and LCFA uptake. *A*, total and phosphorylated PKD and AMPK were detected by immunoblotting and quantified ($n = 4$). These data confirm that the silencing protocols successfully reduced expression and activation of each of the kinases. *B*, PKD1-silenced HL1 cells were used for detection of sarcolemmal GLUT4myc and CD36 contents by a fluorometric assay following cell staining with an HRP-linked secondary antibody ($n = 4$) and also used for measurement of initial uptake rate of [^{3}H]deoxyglucose and [^{14}C]palmitate ($n = 4$). *C*, additionally, PKD1-silenced HL1 cells were used for microscopical visualization of GLUT4 translocation. For this, cells were cotransfected with GLUT4-GFP and after 48 h were subjected to EFS. Translocation of GLUT4-GFP was detected via immunofluorescence microscopy. The nuclei are stained in *blue* (DAPI). Only in the nc-siRNA-transfected cells subjected to EFS, did GLUT4-GFP hybrid proteins move out to the plasma membrane. A representative experiment of three is displayed. *D*, AMPK-silenced HL1 cells were used for detection of sarcolemmal GLUT4myc and CD36 contents as described in *B* ($n = 4$). *, statistically different ($p < 0.05$).

CD36 translocation were total. Both PKD1 and AMPK are known to be involved in a number of pathways not related to regulation of substrate uptake (4, 9). Possibly, variations in thresholds of kinase activity may determine the actual effect of the down-regulation on each of these pathways.

We also investigated the roles of PKD1 and AMPK in contraction-induced glucose and LCFA uptake into primary cardiomyocytes isolated from cardiospecific PKD1 knock-out mice and from AMPKα2 knock-out mice. We confirmed the absence of PKD1 and AMPK activation in cardiomyocytes from cardiospecific PKD1 knock-out mice and from AMPKα2 knock-out mice, respectively (Fig. 2*A*). In PKD1 knock-out cardiomyocytes, EFS-induced AMPK-Thr^{172} phosphorylation was not decreased. Reciprocally, in AMPKα2 knock-out cardiomyocytes, EFS-induced PKD1-Ser^{916} phosphorylation was unaltered (Fig. 2*A*). This latter finding is entirely in line with a previous study in cardiomyocytes from AMPKα2 knock-out mice, showing that the contraction/oligomycin-induced increase in enzymatic PKD1 activity was not impaired compared with cardiomyocytes from wild-type littermates (7). EFS similarly enhanced glucose and LCFA uptake into cardiomyocytes from wild-type littermates of cardiospecific PKD1 knock-out mice and AMPKα2 knock-out mice (Fig. 2*B*). EFS-induced glucose uptake was abolished in both PKD1 knock-out and AMPKα2 knock-out cardiomyocytes (Fig. 2*B*). EFS-induced LCFA uptake was abolished in AMPKα2 knock-out cardiomyocytes but was retained in PKD1 knock-out cardiomyocytes (Fig. 2*B*). Additionally, in PKD1 knock-out cardiomyo-

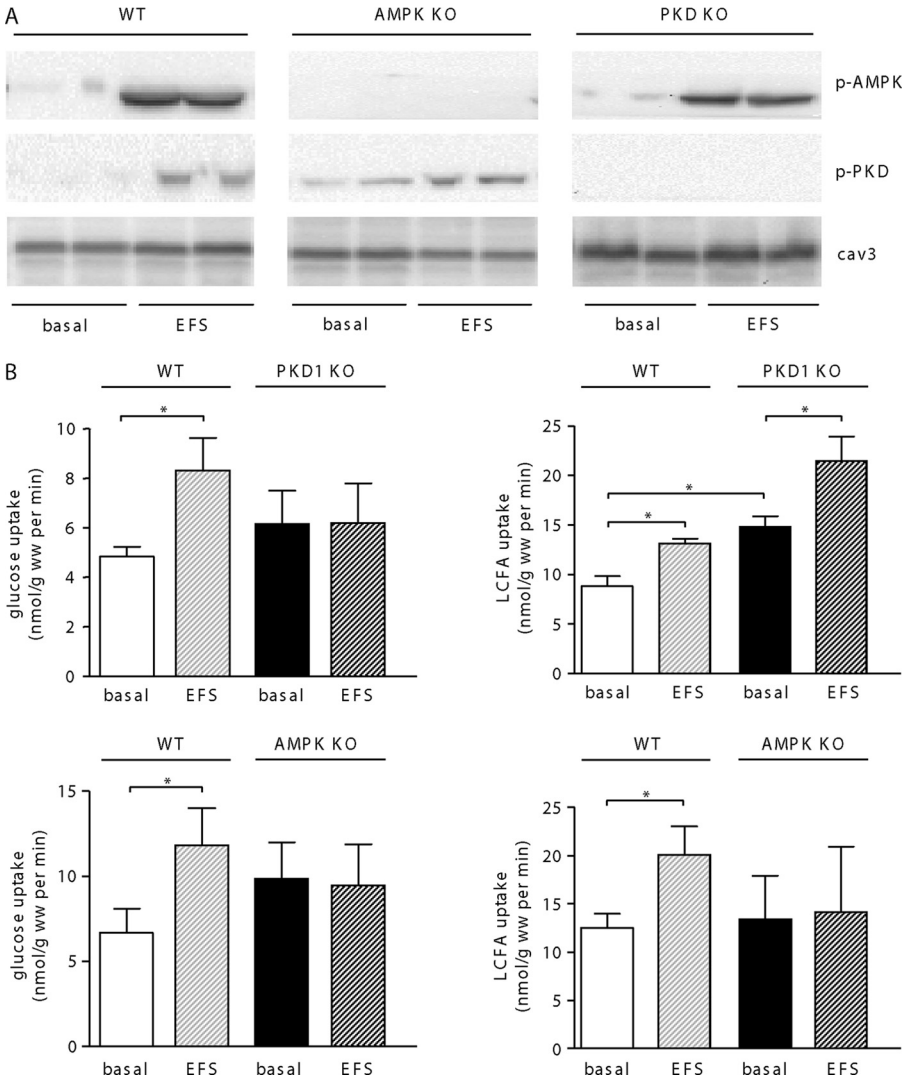

FIGURE 2. **In cardiomyocytes from cardiospecific PKD1 knock-out mice, contraction-induced glucose uptake is lost and LCFA uptake is retained, whereas in cardiomyocytes from AMPKα2 knock-out mice, both contraction-induced glucose and LCFA uptake are lost.** Primary cardiomyocytes from cardiospecific PKD1 knock-out mice ($n = 5$) and AMPKα2 knock-out mice ($n = 5$) and corresponding wild-type littermates ($n = 5$ for both groups) were subjected to 2-Hz EFS prior to measurement of PKD-Ser^{916} and AMPK-Thr^{172} phosphorylation (*A*) or measurement of initial (5 min) uptake of [^{3}H]deoxyglucose and [^{14}C]palmitate (*B*). In *A*, Western blots from wild-type animals are from littermates from AMPKα2 knock-out mice. *, statistically different ($p < 0.05$).

cytes, basal LCFA uptake was enhanced (Fig. 2*B*). Taken together, PKD1 is specifically involved in GLUT4-mediated glucose uptake, whereas AMPK is necessary for both GLUT4-mediated glucose uptake and CD36-mediated LCFA uptake.

Upstream Events of PKD1 in Contraction-induced GLUT4 Translocation and Glucose Uptake—A plausible candidate kinase directly upstream of PKD1 might be death-activated protein kinase (DAPK). This kinase has been found to bind to PKD1 in HEK cells exposed to oxidative stress (13). However, DAPK has never been linked to cardiac glucose utilization. Here, we investigated whether in cardiomyocytes DAPK physically interacts with PKD1 during contraction and whether it mediates GLUT4 translocation. PKD1 was marginally detectable in DAPK immunoprecipitates from cardiomyocytes incubated under basal conditions (Fig. 3*A*). However, DAPK could be easily detected in PKD1 immunoprecipitates from non-stimulated cardiomyocytes (Fig. 3*A*). When cardiomyocytes were subjected to EFS, there was a large increase in the content of PKD1 in DAPK immunoprecipitates (Fig. 3*A*). Reciprocally, EFS induced the presence of DAPK in PKD1 immunoprecipitates (Fig. 3*A*). Hence, there is a physical interaction between DAPK and PKD1 that is augmented by contraction stimulation. In the DAPK immunoprecipitates, the increase in PKD1 content caused by EFS is accompanied by a corresponding increase in Ser^{916}-phosphorylated PKD1 (Fig. 3*A*), suggesting that binding of DAPK to PKD1 upon the onset of contraction leads to PKD1 activation. Knockdown of DAPK (64 $\pm$ 7%) abrogated PKD1 activation (Fig. 3*B*), EFS-induced GLUT4 translocation (Fig. 3*C*), and EFS-induced GLUT4-GFP translocation (Fig. 3*D*). In contrast, CD36 translocation was not affected by DAPK knockdown (Fig. 3*C*). These data indicate that DAPK is necessary for contraction-induced PKD1 activation and subsequent selective stimulation of GLUT4-mediated glucose uptake.

Furthermore, we hypothesized that ROS presents an upstream effector of the PKD1-GLUT4 pathway. In isolated cardiomyocytes, EFS significantly increased ROS formation, as

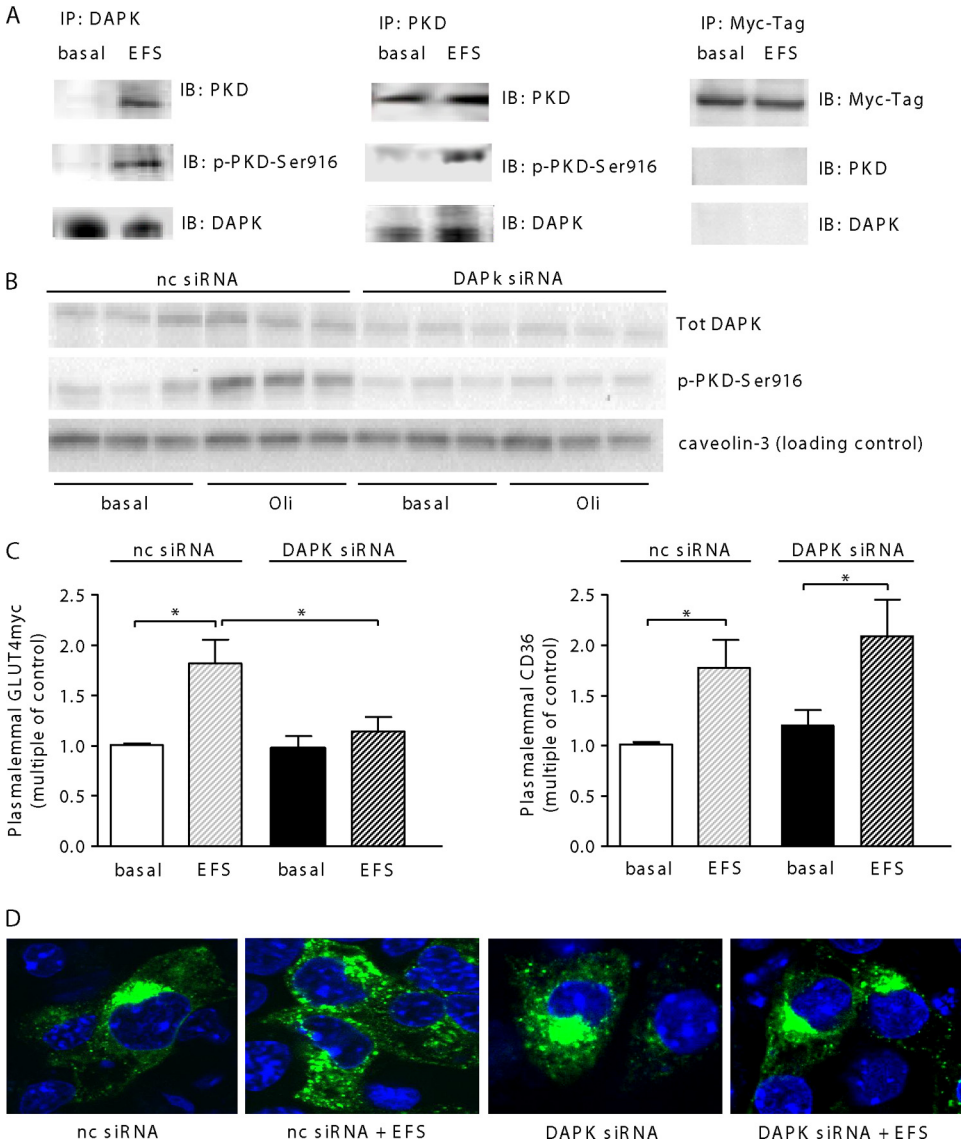

FIGURE 3. **DAPK is involved in PKD1 activation and contraction-induced GLUT4 translocation.** *A*, primary rat cardiomyocytes were treated with or without EFS and subsequently used for immunoprecipitation (*IP*) with monoclonal anti-DAPK or PKD1 antibodies, after which both the DAPK immunoprecipitate and the PKD1 immunoprecipitate were used for immunoblotting (*IB*) against total PKD1 protein expression, phospho-PKD-Ser^{916}, and total DAPK protein expression. In a control immunoprecipitation of cardiomyocytes lysates with a Myc tag antibody, the endogenous c-Myc protein (65 kDa) was successfully immunoprecipitated, whereas there was no detectable coimmunoprecipitation of DAPK and PKD1. Representative blots are shown ($n = 3$). *B* and *C*, HL1 cardiomyocytes were transfected with nc- or DAPK-siRNA and cotransfected with pCMV-GLUT4myc (in case of sarcolemmal GLUT4 detection) and after 48 h were treated with oligomycin (*Oli*; 1 μM, 30 min) or subjected to EFS. In *B*, DAPK expression and PKD1-Ser^{916} phosphorylation were detected by IB ($n = 4$), and in *C*, sarcolemmal GLUT4myc and CD36 content were detected by a fluorometric assay following cell staining with an HRP-linked secondary antibody ($n = 4$). *D*, additionally, nc-siRNA-treated or DAPK-silenced cells were cotransfected with GLUT4 GFP and after 48 h were subjected to EFS for immunofluorescence detection of GLUT4 translocation. The nuclei are stained in *blue* (DAPI). Only in the nc-siRNA-transfected cells subjected to EFS, GLUT4-GFP hybrid proteins move out to the plasma membrane. A representative experiment of three is displayed. *, statistically different ($p < 0.05$).

did oligomycin (Fig. 4*A*). Subsequently, we investigated the ability of ROS to induce PKD1 activation and glucose uptake and, for comparison, AMPK activation and LCFA uptake. Indeed, H_2O_2-induced ROS formation in cardiomyocytes substantially enhanced PKD1-Ser^{916} phosphorylation as well as AMPK-Thr^{172} phosphorylation (Fig. 4*B*). H_2O_2 treatment also enhanced both glucose and LCFA uptake (Fig. 4*C*). To investigate whether PKD1 and AMPK are involved in these stimulatory actions of H_2O_2 on substrate uptake, we used the staurosporin-derivative Ro318220, which has been routinely used to inhibit PKD activation (14) and also adenine 9-β-D-arabinofuranoside (ara-A), an established AMPK inhibitor (15). We confirmed that Ro318220 blocked PKD1 but not AMPK activation and that ara-A blocked AMPK activation but not PKD1 activation (supplemental Figs. S1*A* and S2). H_2O_2-induced glucose uptake, but not H_2O_2-induced LCFA uptake, was blunted by Ro318220, whereas both H_2O_2-induced glucose and LCFA uptake were blocked by ara-A treatment (Fig. 4*C*). This pattern of inhibition of H_2O_2-induced substrate uptake by Ro318220 and ara-A closely resembled that of oligomycin/EFS-induced glucose and LCFA uptake into cardiomyocytes (supplemental Fig. S1*B*), suggesting a common mechanism. To obtain kinetic evidence whether H_2O_2 treatment uses the same mechanisms as oligomycin or EFS to enhance substrate uptake into car-

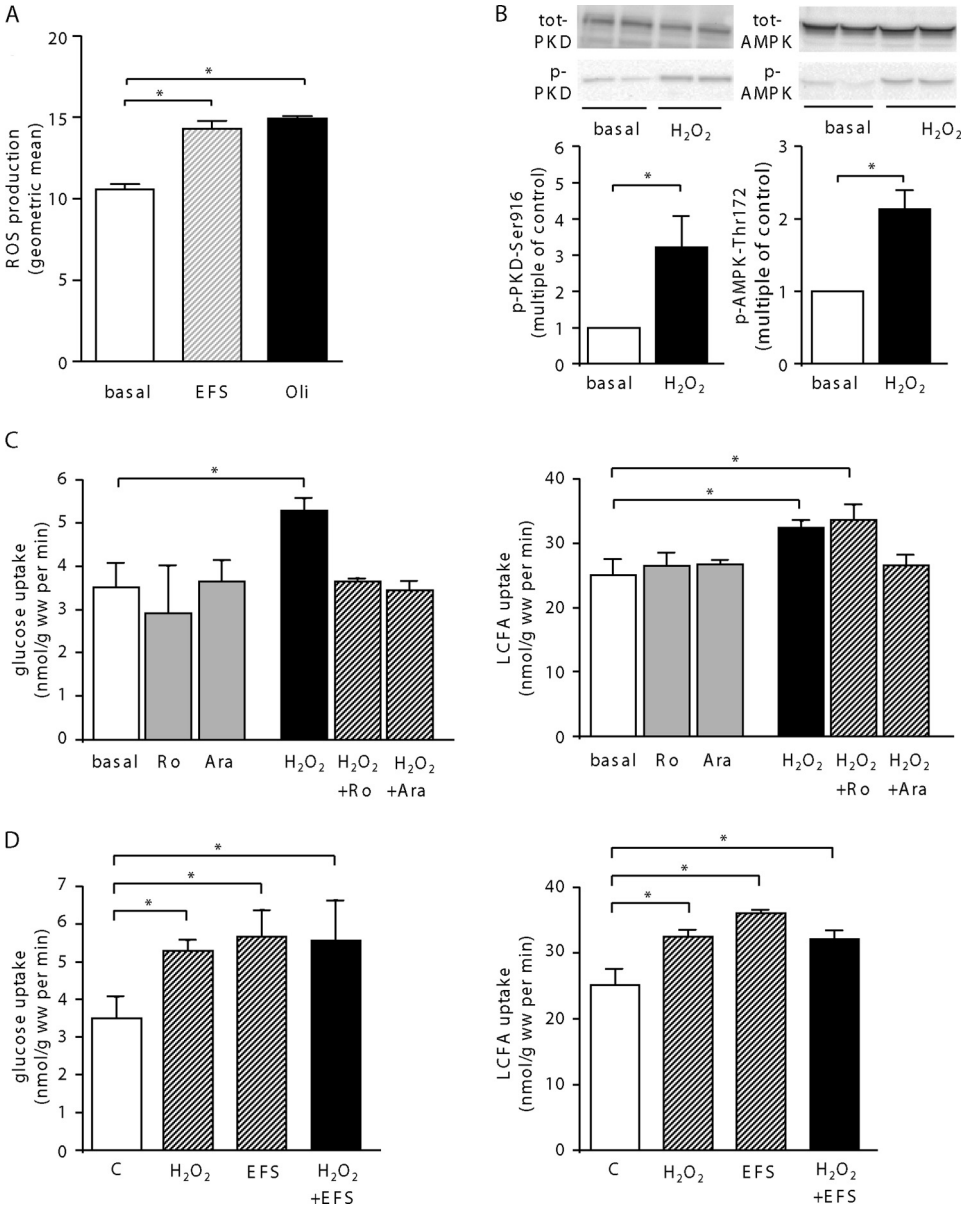

FIGURE 4. **Similarly to contraction stimulation, H_2O_2-induced ROS formation activates PKD1 and AMPK and stimulates glucose and LCFA uptake into primary cardiomyocytes.** *A* and *B*, primary rat cardiomyocytes were treated with oligomycin (*Oli*; 5 μM; 15 min), 4-Hz EFS, or with the ROS donor H_2O_2 (10 μM; 10 min) prior to measurement of ROS production ($n = 4$) (*A*), measurement of PKD1-Ser^{916} and AMPK-Thr^{172} phosphorylation ($n = 5$) (*B*), and measurement of initial (5 min) uptake of [^{3}H]deoxyglucose and [^{14}C]palmitate ($n = 4$) (*C* and *D*). In *C*, cardiomyocytes were preincubated with Ro318220 (*Ro*, 10 μM; 30 min) or ara-A (*Ara*, 3 mM; 15 min) prior to H_2O_2 treatment. In *D*, cardiomyocytes were simultaneously subjected to EFS and treated with H_2O_2. *, statistically different ($p < 0.05$).

diomyocytes, we investigated the degree of additivity of H_2O_2-induced glucose and LCFA uptake with EFS-induced glucose and LCFA uptake, respectively. H_2O_2 treatment and EFS each enhanced glucose and LCFA uptake into cardiomyocytes, but their combined action did not further enhance glucose and LCFA uptake (Fig. 4*D*). This lack of additivity indicates a common underlying mechanism.

To demonstrate a direct causal relationship between contraction-induced ROS production, PKD1 activation, and glucose uptake, we used the ROS scavenger MPG (16). At 0.15 mM, MPG markedly decreased oligomycin-induced PKD1-Ser^{916} phosphorylation but did not affect AMPK-Thr^{172} phosphorylation (Fig. 5*A*). However, at 1 mM MPG, both phosphorylation events were largely reduced (Fig. 5*A*). Additionally, 0.15 mM MPG largely blocked oligomycin/EFS-induced glucose uptake without affecting EFS-induced LCFA uptake, whereas 1 mM MPG blocked oligomycin/EFS-induced LCFA uptake as well (Fig. 5*B*). Hence, ROS is involved in contraction-induced PKD1 and AMPK activation as well as in contraction-induced glucose and LCFA uptake. However, contraction-induced PKD1 activation and glucose uptake are more sensitive to decreases in intracellular ROS concentrations than contraction-induced AMPK activation and LCFA uptake.

DISCUSSION

This study was aimed at investigating the role of PKD1, in relation to AMPK, in regulating substrate uptake into contracting cardiomyocytes, and also aimed at elucidating the upstream

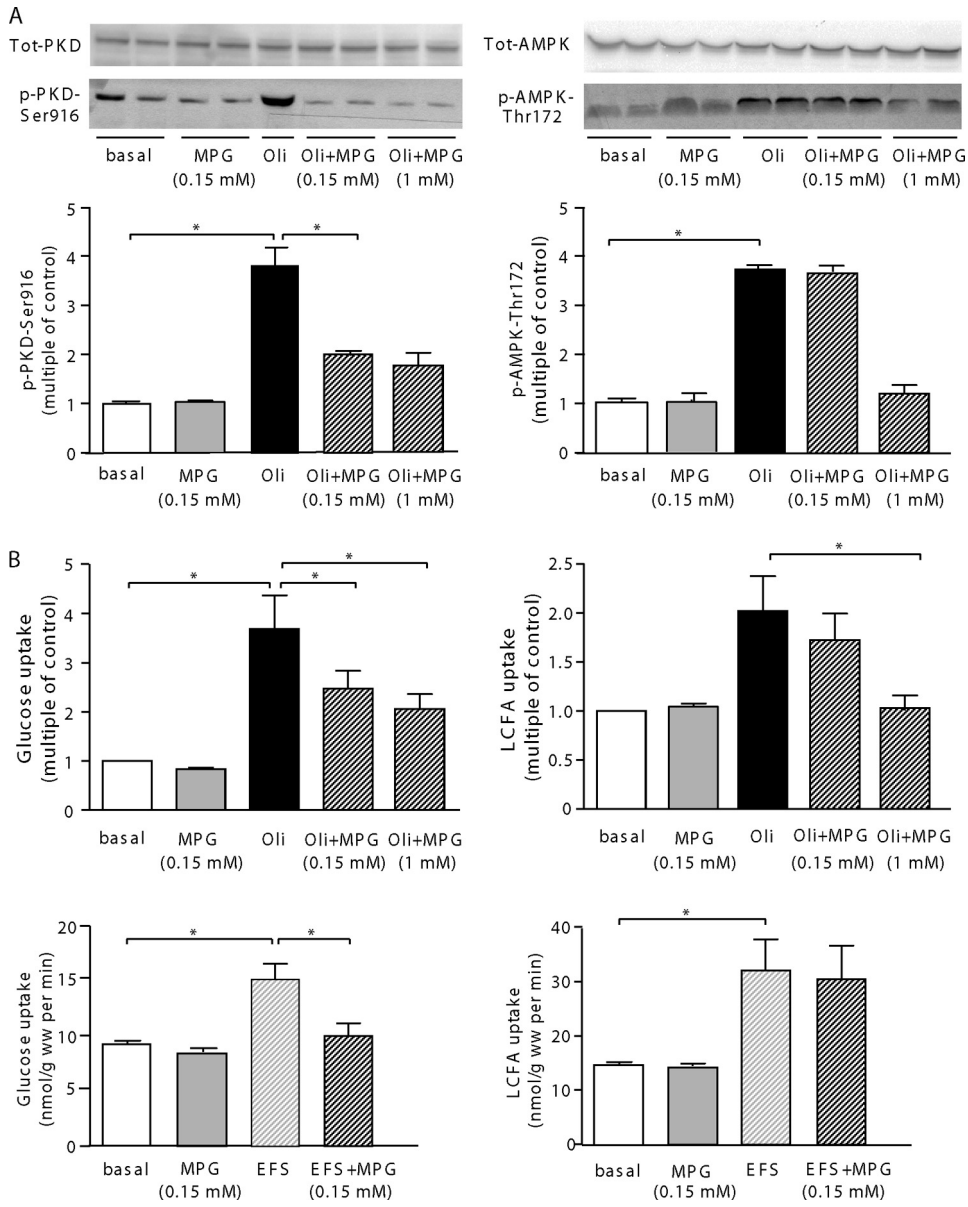

FIGURE 5. **PKD1 activation and stimulation of glucose uptake into primary cardiomyocytes display a greater sensitivity toward ROS scavenging than AMPK activation and stimulation of LCFA uptake.** Primary rat cardiomyocytes were preincubated in absence or presence of indicated concentrations of the ROS scavenger MPG (30 min) and subsequently treated with oligomycin (*Oli*; 5 μM; 15 min) or EFS prior to Western detection of PKD-Ser^{916} and AMPK-Thr^{172} phosphorylation ($n = 4$) (*A*) or measurement of initial uptake of [^{3}H]deoxyglucose and [^{14}C]palmitate ($n = 4$) (*B*). *, statistically different ($p < 0.05$).

events responsible for contraction-induced PKD1 activation. The presented results yielded the following novel insights: (i) PKD1 is specifically involved in contraction-induced glucose uptake, unlike AMPK, being involved in both contraction-induced glucose and LCFA uptake; (ii) the upstream events in contraction-induced PKD1 activation may include ROS production and binding of PKD1 to DAPK; and (iii) PKD1 and AMPK are activated via separate contraction-induced pathways, but activation of both kinases is necessary for GLUT4 translocation.

PKD1 Is Specifically Involved in Contraction-induced Glucose Uptake—In the present study, we obtained three sets of data that PKD1 is not involved in CD36 translocation and hence specifically mediates contraction-induced GLUT4 translocation: (i) in primary cardiomyocytes from cardiospecific PKD1 knock-out mice, contraction-induced glucose uptake was abolished, whereas contraction-induced LCFA uptake was unimpaired; (ii) in HL1 cardiomyocytes, PKD1 silencing inhibited contraction-induced glucose uptake but had no effect on contraction-induced LCFA uptake; and (iii) in primary rat cardiomyocytes pharmacological PKD inhibition inhibited contraction-induced glucose uptake but not LCFA uptake (supplemental Fig. S1). On the other hand, AMPK activation is involved in both GLUT4 and CD36 translocation in cardiomyocytes. First, in rat cardiomyocytes, AMPK-activating stimuli induce translocation of both GLUT4 and CD36 (1, 3), and in cardiomyocytes from dominant-negative AMPK expressing mice (17), both contraction-induced glucose and LCFA uptake are abolished (6). Moreover, in the present study, we observed that in AMPK-silenced HL1 cells and in cardiomyocytes from

AMPKα2 mice, both contraction-induced GLUT4-mediated glucose uptake and CD36-mediated LCFA uptake were abolished.

In addition to effects on EFS/oligomycin-induced glucose and/or LCFA uptake, silencing or knock-out of PKD1 or AMPK can also affect basal substrate uptake. In AMPK-silenced cells, there is a trend to an increased basal GLUT4 and CD36 translocation. This suggests that neutralization of AMPK leads to the activation of compensatory mechanisms, which increases both basal glucose and LCFA. In PKD1 KO cardiomyocytes, the LCFA uptake rate is higher in both basal and EFS conditions. The increase in LCFA uptake observed in PKD1 KO cardiomyocytes suggests that PKD1 is able to inhibit LCFA uptake.

Upstream Events in Contraction-induced PKD1 Activation—In search of an upstream kinase mediating PKD1 activation in cardiomyocytes and subsequent GLUT4 translocation, we speculated on the involvement of DAPK. Namely, DAPK has been shown in HEK cells to physically interact with and to activate PKD1 in response to oxidative stress (13). However, DAPK is mainly known as a tumor suppressor, the expression of which is greatly reduced in various human malignancies (18, 19). Until now, no metabolic actions have been assigned to DAPK. We first studied whether DAPK would also physically interact with PKD1 in cardiomyocytes. PKD1 is marginally present in DAPK immunoprecipitates from nonstimulated cardiomyocytes, suggesting that the degree of physical interaction between both proteins under basal conditions is low. However, in these same cells DAPK is easily detectable in PKD1 immunoprecipitates, for which we do not yet have a plausible explanation. More importantly, the onset of contraction enhances binding of DAPK to PKD1 in cardiomyocytes. Additionally, the increase in total PKD content in DAPK immunoprecipitates upon contraction stimulation is closely mirrored by an increase in Ser^{916}-autophosphorylated (and hence activated) PKD in these precipitates. This implicates that DAPK-PKD1 binding and PKD1 activation are associated events. Silencing of DAPK further illustrates its essential role in contraction-induced PKD1 activation, because oligomycin did not result in autophosphorylation of PKD1 in DAPK-depleted HL1 cells. Hence, DAPK is needed for PKD1 autophosphorylation. Combined with the contraction-stimulated binding of total and Ser^{916}-phosphorylated PKD1 to DAPK, this finding indicates that upon contraction DAPK increases its affinity for nonphosphorylated PKD1 and activates it upon binding. The mechanism of how DAPK is activated by contraction is not known. DAPK silencing also abrogated contraction-induced GLUT4 translocation, thereby adding DAPK to the list of kinases involved in GLUT4 translocation. Thus, not only PKD1 silencing but also silencing of its upstream kinase resulted in a loss of contraction-induced GLUT4 translocation. In contrast, DAPK silencing did not affect contraction-induced CD36 translocation, which is in line with the noninvolvement of PKD1 herein. Taken together, we have unmasked a novel DAPK-PKD1 axis that is specifically involved in contraction-induced GLUT4 translocation and glucose uptake.

In search of a second messenger mediating PKD1 activation and subsequent GLUT4 translocation, we hypothesized that ROS might be involved. Namely, it has been shown that the induction of contraction enhances ROS formation in cardiomyocytes (20) and that ROS scavengers inhibit contraction-induced glucose uptake (21, 22). Furthermore, PKD1 is known to be activated by mitochondrial ROS (9). In the present study, we confirmed that EFS-induced contraction enhances ROS formation in cardiomyocytes. Also, induced ROS formation in H_2O_2-treated cardiomyocytes resulted in Ser^{916} phosphorylation and activation of PKD1. On the other hand, ROS scavenging with relatively modest concentrations MPG inhibited PKD1 activation as well as glucose uptake. AMPK has also been reported to be activated by a rise in intracellular ROS through AMPK-Thr^{172} phosphorylation (23). However, only high concentrations of MPG (1 mM) provided sufficient scavenging to block AMPK activation. This shows that although both PKD1 and AMPK are activated by ROS, these kinases differ in their sensitivity to ROS. Pharmacological inhibition of AMPK blocked both ROS-induced glucose and LCFA uptake, whereas inhibition of PKD1 selectively abrogated ROS-induced glucose uptake. Hence, enhanced ROS formation has similar effects on signaling and substrate uptake as EFS and oligomycin-induced contraction, suggesting that ROS is involved in contraction-induced glucose as well as LCFA uptake. This notion is further strengthened by the nonadditivity of ROS-induced glucose and LCFA uptake with contraction-induced glucose and LCFA uptake.

In conclusion, ROS and DAPK are both upstream factors mediating PKD1 activation in contracting cardiomyocytes. Elucidation of the molecular mechanism of interplay among ROS, DAPK, and PKD1 that leads to PKD1 activation is a topic for further study.

Both PKD1 and AMPK Activation Are Necessary for Contraction-induced GLUT4 Translocation—Contraction-induced GLUT4 translocation is abrogated by either PKD1-knockdown/knock-out or AMPK-knockdown/knock-out. Hence, both kinases need to be activated for GLUT4 translocation. The data obtained in this study indicate that PKD1 and AMPK do not operate in the same signal transduction pathway to mediate contraction-induced GLUT4 translocation. Rather they act parallel to each other, in separate pathways. Evidence for this concept includes: (i) in PKD1-silenced cells or cardiomyocytes derived from PKD1 knock-out mice, AMPK activation was unimpaired, and, reciprocally, in AMPK-silenced cells or cardiomyocytes from AMPK knock-outs, PKD1 activation was not decreased; (ii) pharmacological inhibition of PKD1 activation did not affect H_2O_2-induced AMPK activation, because pharmacological AMPK inhibition did not affect H_2O_2-induced PKD1 activation; (iii) upon modest (0.15 mM) MPG treatment, PKD1 activation was inhibited, whereas AMPK activation was unimpaired; and (iv) AICAR is an established AMPK activator that stimulates LCFA uptake but does not alter glucose uptake (supplemental Fig. S3) or PKD1 phosphorylation (effect of AICAR on PKD-Ser^{916} phosphorylation compared with basal: 1.02 ± 0.05; $n = 4$). This inability of AICAR to stimulate glucose uptake is in contrast to observations in skeletal muscle (24), suggesting that similarities in regulation of GLUT4 translocation exist between heart and muscle.

This combined evidence that both PKD1 and AMPK appear to be necessary for GLUT4 translocation but operate separately from each other suggests that contraction-induced GLUT4 translocation requires the combined input of two separate contraction-activated pathways, one involving AMPK and its

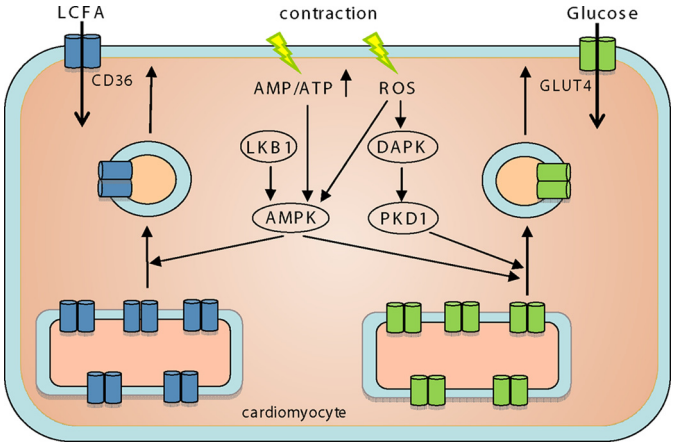

FIGURE 6. **Schematic presentation of the ROS-DAPK-PKD1-GLUT4 axis as a novel pathway involved in contraction-induced glucose but not LCFA uptake.** Upon contraction, both GLUT4 and CD36 are translocated from intracellular stores to the sarcolemma through a vesicle-mediated process. Whereas contraction-induced GLUT4 translocation depends on both AMPK and PKD1 activation, contraction-induced CD36 translocation requires AMPK, but not PKD1 activation. AMPK and PKD1 are activated upon contraction via separate signaling pathways. An increase in the AMP/ATP ratio enables LKB1 to activate AMPK. Additionally, AMPK activation is supported by ROS formation. Furthermore, increased ROS production and DAPK binding to PKD1 are upstream events for PKD1 activation. Remarkably, not only is PKD1 directly activated by a tumor suppressor (*i.e.* DAPK), but also LKB1, the upstream kinase of AMPK, is known to be a tumor suppressor. Hence, there is a striking symmetry in AMPK and PKD signaling toward GLUT4 translocation. Specifically, inactivation of LKB1 is involved in the development of the Peutz-Jeghers syndrome (29).

upstream activating kinase LKB1 (4, 6), the other involving PKD1 and its upstream kinase DAPK. These two pathways are simultaneously activated upon increased contractile activity through enhanced ATP utilization and oxidative phosphorylation, resulting in the simultaneous formation of AMP and ROS, the second messengers for these respective pathways (Fig. 6). In the present study, we have not investigated intracellular AMP levels, but earlier we observed a 2-fold increase in intracellular AMP upon 4-Hz contraction (3, 6). This dual signaling input for contraction-induced GLUT4 translocation is in line with studies in skeletal muscle demonstrating that AMPK is essential but not sufficient for contraction-induced GLUT4 translocation and glucose uptake (25, 26). On the other hand, another study in skeletal muscle showed that contraction-induced GLUT4 translocation was found to be dependent on ROS signaling and independent of AMPK activation (21). Hence, further studies are needed to study the combined roles of ROS and AMPK signaling in skeletal muscle.

One can only speculate at which site both contraction-activated signaling pathways converge to induce GLUT4 translocation. Downstream targets of AMPK signaling are AS160 and/or its closely related family member TBC1D1. Their phosphorylation has been shown to relieve GLUT4 from retention within the recycling endosomes (27). This AMPK signaling-induced removal of the brake on GLUT4 translocation apparently is not sufficient for initiation of GLUT4 translocation. Thus, an extra PKD1-dependent input signal is necessary to induce excision of GLUT4-containing vesicles from the endosomal compartment for translocation to the sarcolemma. Then this raises the question as to how PKD1 signals to endosomes for induction of GLUT4 translocation. More than 1,000 proteins have been shown to possess a PKD consensus phosphorylation motif. Among these proteins are several Golgi-associated proteins (*e.g.* diacylglycerol kinase, phosphatidylinositol 4-kinase IIIβ, and the acyl transferase CtBP3/BARS), which function in vesicle-mediated transport between the Golgi and the plasma membrane (28). Because the Golgi and the recycling endosomes are not distinct entities and have multiple membranous connections, several of these PKD1 consensus phosphorylation motif-possessing proteins of the Golgi could also be present within the recycling endosomes. One of these proteins could then be specifically involved in vesicle-mediated transport of GLUT4 from the recycling endosomes to the sarcolemma and might cooperate with AS160 to complete the contraction-induced excision of GLUT4 vesicles. Such a combined input of two separate signaling pathways may serve as a control mechanism to safeguard that GLUT4 translocation will be initiated under the appropriate metabolic conditions.

In conclusion, in cardiomyocytes, a contraction-activated ROS-DAPK-PKD1 pathway induces GLUT4 but not CD36 translocation. Selective activation of this pathway may shift cardiac substrate preference toward glucose. Furthermore, selective stimulation of glucose uptake might be beneficial for hearts from type 2 diabetic individuals, which are characterized by chronically increased LCFA uptake, excessive lipid accumulation, and loss of glucose utilization (1). This selective stimulation of glucose uptake may compensate for the decreased contractile potential of the diabetic heart.

Acknowledgments—PKD1 knock-out mice were a gift from Prof. E. N. Olson (University of Texas Southwestern Medical Center, Dallas, TX). The authors acknowledge the technical support of Dr. Jos Broers (Department of Cell Biology, Maastricht University) and the students Laura Schmidt and Annemarie Güntsch in performing the microscopical experiments.

REFERENCES

1. Glatz, J. F., Luiken, J. J., and Bonen A. (2010) Membrane fatty acid transporters as regulators of lipid metabolism. Implications for metabolic disease. *Physiol. Rev.* **90,** 367–417
2. Schwenk, R. W., Dirkx, E., Coumans, W. A., Bonen, A., Klip, A., Glatz, J. F., and Luiken, J. J. (2010) Requirement for distinct vesicle-associated membrane proteins in insulin- and AMP-activated protein kinase (AMPK)-induced translocation of GLUT4 and CD36 in cultured cardiomyocytes. *Diabetologia* **53,** 2209–2219
3. Luiken, J. J., Coort, S. L., Willems, J., Coumans, W. A., Bonen, A., van der Vusse, G. J., and Glatz, J. F. (2003) Contraction-induced fatty acid translocase/CD36 translocation in rat cardiac myocytes is mediated through AMP-activated protein kinase signaling. *Diabetes* **52,** 1627–1634
4. Hardie, D. G., Hawley, S. A., and Scott, J. W. (2006) AMP-activated protein kinase. Development of the energy sensor concept. *J. Physiol.* **574,** 7–15
5. Kurth-Kraczek, E. J., Hirshman, M. F., Goodyear, L. J., and Winder, W. W. (1999) 5′ AMP-activated protein kinase activation causes GLUT4 translocation in skeletal muscle. *Diabetes* **48,** 1667–1671
6. Habets, D. D., Coumans, W. A., El Hasnaoui, M., Zarrinpashneh, E., Bertrand, L., Viollet, B., Kiens, B., Jensen, T. E., Richter, E. A., Bonen, A., Glatz, J. F., and Luiken, J. J. (2009) Crucial role for LKB1 to AMPKα2 axis in the regulation of CD36-mediated long-chain fatty acid uptake into cardiomyocytes. *Biochim. Biophys. Acta* **1791,** 212–219
7. Luiken J. J., Vertommen, D., Coort, S. L., Habets, D. D., El Hasnaoui, M., Pelsers, M. M., Viollet, B., Bonen, A., Hue, L., Rider, M. H., and Glatz, J. F. (2008) Identification of protein kinase D as a novel contraction-activated

kinase linked to GLUT4-mediated glucose uptake, independent of AMPK. *Cell Signal.* **20,** 543–556
8. Hausser, A., Storz, P., Märtens, S., Link, G., Toker, A., and Pfizenmaier, K. (2005) Protein kinase D regulates vesicular transport by phosphorylating and activating phosphatidylinositol-4 kinase IIIβ at the Golgi complex. *Nat. Cell Biol.* **7,** 880–886
9. Storz, P. (2007) Mitochondrial ROS. Radical detoxification, mediated by protein kinase D. *Trends Cell Biol.* **17,** 13–18
10. Viollet, B., Andreelli, F., Jørgensen, S. B., Perrin, C., Geloen, A., Flamez, D., Mu, J., Lenzner, C., Baud, O., Bennoun, M., Gomas, E., Nicolas, G., Wojtaszewski, J. F., Kahn, A., Carling, D., Schuit, F. C., Birnbaum, M. J., Richter, E. A., Burcelin, R., and Vaulont, S. (2003) The AMP-activated protein kinase α2 catalytic subunit controls whole-body insulin sensitivity. *J. Clin. Invest.* **111,** 91–98
11. Wang, Q., Khayat, Z., Kishi, K., Ebina, Y., and Klip, A. (1998) GLUT4 translocation by insulin in intact muscle cells: detection by a fast and quantitative assay. *FEBS Lett.* **427,** 193–197
12. Luiken, J. J., van Nieuwenhoven, F. A., America, G., van der Vusse, G. J., and Glatz, J. F. (1997) Uptake and metabolism of palmitate by isolated cardiac myocytes from adult rats. Involvement of sarcolemmal proteins. *J. Lipid Res.* **38,** 745–758
13. Eisenberg-Lerner, A., and Kimchi, A. (2007) DAP kinase regulates JNK signaling by binding and activating protein kinase D under oxidative stress. *Cell Death Differ.* **14,** 1908–1915
14. Zugaza, J. L., Sinnett-Smith, J., Van Lint, J., and Rozengurt, E. (1996) Protein kinase D (PKD) activation in intact cells through a protein kinase C-dependent signal transduction pathway. *EMBO J.* **15,** 6220–6230
15. Musi, N., Hayashi, T., Fujii, N., Hirshman, M. F., Witters, L. A., and Goodyear, L. J. (2001) AMP-activated protein kinase activity and glucose uptake in rat skeletal muscle. *Am. J. Physiol. Endocrinol. Metab.* **280,** E677–E684
16. De Giusti, V. C., Garciarena, C. D., and Aiello, E. A. (2009) Role of reactive oxygen species (ROS) in angiotensin II-induced stimulation of the cardiac Na^+/HCO_3^- cotransport. *J. Mol. Cell Cardiol.* **47,** 716–722
17. Zong, H., Ren, J. M., Young, L. H., Pypaert, M., Mu, J., Birnbaum, M. J., and Shulman, G. I. (2002) AMP kinase is required for mitochondrial biogenesis in skeletal muscle in response to chronic energy deprivation. *Proc. Natl. Acad. Sci. U.S.A.* **99,** 15983–15987
18. Levy-Strumpf, N., and Kimchi, A. (1998) Death associated proteins (DAPs). From gene identification to the analysis of their apoptotic and tumor suppressive functions. *Oncogene* **17,** 3331–3340
19. Ng, M. H. (2002) Death associated protein kinase. From regulation of apoptosis to tumor suppressive functions and B cell malignancies. *Apoptosis* **7,** 261–270
20. Heinzel, F. R., Luo, Y., Dodoni, G., Boengler, K., Petrat, F., Di Lisa, F., de Groot, H., Schulz R., and Heusch, G. (2006) Formation of reactive oxygen species at increased contraction frequency in rat cardiomyocytes. *Cardiovasc. Res.* **71,** 374–382
21. Merry, T. L., Steinberg, G. R., Lynch, G. S., and McConell, G. K. (2010) Skeletal muscle glucose uptake during contraction is regulated by nitric oxide and ROS independently of AMPK. *Am. J. Physiol. Endocrinol. Metab.* **298,** E577–E585
22. Smith, M. A., and Reid, M. B. (2006) Redox modulation of contractile function in respiratory and limb skeletal muscle. *Respir. Physiol. Neurobiol.* **151,** 229–241
23. Horie, T., Ono, K., Nagao, K., Nishi, H., Kinoshita, M., Kawamura, T., Wada, H., Shimatsu, A., Kita, T., and Hasegawa, K. (2008) Oxidative stress induces GLUT4 translocation by activation of PI3-K/Akt and dual AMPK kinase in cardiac myocytes. *J. Cell Physiol.* **215,** 733–742
24. Merrill, G. F., Kurth, E. J., Hardie, D. G., and Winder, W. W. (1997) AICA riboside increases AMP-activated protein kinase, fatty acid oxidation, and glucose uptake in rat muscle. *Am. J. Physiol.* **273,** E1107–E1112
25. Fujii, N., Hirshman, M. F., Kane, E. M., Ho, R. C., Peter, L. E., Seifert, M. M., and Goodyear, L. J. (2005) AMP-activated protein kinase α2 activity is not essential for contraction- and hyperosmolarity-induced glucose transport in skeletal muscle. *J. Biol. Chem.* **280,** 39033–39041
26. Lefort, N., St-Amand, E., Morasse, S., Côté, C. H., and Marette, A. (2008) The α-subunit of AMPK is essential for submaximal contraction-mediated glucose transport in skeletal muscle in vitro. *Am. J. Physiol. Endocrinol. Metab.* **295,** E1447–E1454
27. Taylor, E. B., An, D., Kramer, H. F., Yu, H., Fujii, N. L., Roeckl, K. S., Bowles, N., Hirshman, M. F., Xie, J., Feener, E. P., and Goodyear, L. J. (2008) Discovery of TBC1D1 as an insulin-, AICAR-, and contraction-stimulated signaling nexus in mouse skeletal muscle. *J. Biol. Chem.* **283,** 9787–9796
28. Ghanekar, Y., and Lowe, M. (2005) Signalling for secretion. *Nat. Cell Biol.* **7,** 851–853
29. Hemminki, A., Markie, D., Tomlinson, I., Avizienyte, E., Roth, S., Loukola, A., Bignell, G., Warren, W., Aminoff, M., Höglund, P., Järvinen, H., Kristo, P., Pelin, K., Ridanpää, M., Salovaara, R., Toro, T., Bodmer, W., Olschwang, S., Olsen, A. S., Stratton, M. R., de la Chapelle, A., and Aaltonen, L. A. (1998) A serine/threonine kinase gene defective in Peutz-Jeghers syndrome. *Nature* **391,** 184–187